

cm^{-1} , the region of the spectra expected for N-H stretching vibrations. It is of interest to note that $[(\text{Me}_3\text{SiCH}_2)_2\text{AlN}(\text{Me})\text{H}]_2$ has been reported to exist as the trans isomer with only a single proton resonance for the methylene protons of CH_2SiMe_3 .⁴

In summary, a comparison of data for the series of compounds AlR_3 , AlR_2H , AlR_2Br , R_2AlPPh_2 , and $\text{R}_2\text{AlN}(\text{Me})\text{H}$ demonstrates that neopentyl derivatives are less associated than (trimethylsilyl)methyl derivatives if they are electron-deficient but more associated if they are electron-precise. Presumably for electron-deficient compounds withdrawal of electron density from the bridging unit is the dominant factor influencing the degree of association, whereas for electron-precise compounds where

there are plenty of electrons, the enhanced Lewis acidity of the aluminum is most important.

Acknowledgment. This work was supported in part by the Office of Naval Research and by a postdoctoral fellowship from the Alfa Products Division of Morton Thiokol, Inc. (L.V.).

Registry No. AlBr_3 , 7727-15-3; $\text{LiCH}_2\text{CMe}_3$, 7412-67-1; $\text{Al}(\text{CH}_2\text{CMe}_3)_3$, 42916-36-9; $\text{LiAl}(\text{CH}_2\text{CMe}_3)_4$, 110638-20-5; $\text{Al}(\text{CH}_2\text{CMe}_3)_2\text{Br}$, 110638-23-8; $\text{Al}(\text{CH}_2\text{CMe}_3)_2\text{H}$, 65514-51-4; $(\text{Me}_3\text{CCH}_2)_3\text{Al-PPh}_2\text{H}$, 110638-21-6; $(\text{Me}_3\text{CCH}_2)_2\text{AlPPh}_2$, 110638-24-9; CMe_4 , 463-82-1; KPPPh_2 , 15475-27-1; $(\text{Me}_3\text{CCH}_2)_3\text{Al-N}(\text{Me})\text{H}_2$, 110638-22-7; $(\text{Me}_3\text{CCH}_2)_2\text{AlN}(\text{Me})\text{H}$, 110638-25-0.

Electron Transfer from Borohydride and Selective Reductions of Iron Cations. Synthesis of Tetrathiooxalate Iron Derivatives

Daniel Touchard, Jean-Luc Fillaut, Dilip V. Khasnis, and Pierre H. Dixneuf*

Laboratoire de Chimie de Coordination Organique, UA CNRS 415, Université de Rennes, Campus de Beaulieu, 35042 Rennes Cedex, France

Carlo Mealli and Dante Masi

Istituto per la Studio della Stereochimica ed Energetica dei Composti di coordinazione del CNR, 50132 Firenze, Italy

Loïc Toupet

Laboratoire de Physique Cristalline, UA CNRS 804, Université de Rennes, Campus de Beaulieu, 35042 Rennes Cedex, France

Received April 16, 1987

Cations of the type $\text{Fe}(\eta^2\text{-CS}_2\text{R})(\text{CO})_2(\text{L})_2^+$ ($\text{L} = \text{PPh}_3$; $\text{R} = \text{Me}$ (**2a**), Et (**2b**), $\text{CH}_2\text{C}(\text{Me})=\text{CH}_2$ (**2c**)) react with NaBH_4 to afford, via electron transfer, C-C coupling products $(\text{RS})_2\text{C}_2\text{S}_2\text{Fe}_2(\text{CO})_4(\text{L})_2$ (**3a-c**). Complexes **2** containing an acylalkyl group, **R**, also give complexes **3d,e**, but only on reduction with activated magnesium. Reduction of cations **2a-c** with sodium amalgam leads first to **3a-c** and then to the $(\text{RS})_2\text{C}_2\text{S}_2\text{Fe}(\text{CO})_2(\text{L})$ complexes (**4**). Complexes **4a-c** are also obtained on treatment of **3a-c** with Lewis acids in the presence of air. Cation **2h** ($\text{L} = \text{P}(\text{OMe})_3$, $\text{R} = \text{Me}$) is less easily reduced ($E_c = -0.81$ V vs SCE) than **2a** ($\text{L} = \text{PPh}_3$; $E_c = -0.74$ V vs SCE) and, when treated with NaBH_4 , undergoes electron transfer and hydride addition: complex **6**, analogous to **3**, and $\text{Fe}(\eta^2\text{-HCS}_2\text{Me})(\text{CO})_2\text{L}_2$ (**5**) are thus formed. Reaction of **2h** with Na/Hg affords by contrast small amounts of $\text{FeCS}(\text{CO})_2\text{L}_2$ (**8**) and $(\text{R}_2\text{S})_2\text{C}_2\text{S}_2\text{Fe}(\text{CO})\text{L}_2$ (**9**). The X-ray diffraction structures of **3a** and **4a** have been determined. **3a**: space group $\overline{P}1$, $Z = 2$, $a = 9.669$ (2) Å, $b = 13.477$ (3) Å, $c = 17.323$ (3) Å, $\alpha = 101.1$ (2)°, $\beta = 91.5$ (2)°, $\gamma = 110.3$ (2)°, $V = 2048$ Å³, $R = 0.058$ for 3802 reflections having $I > \sigma(I)$. **4a**: space group $P2_1/a$, $Z = 4$, $a = 24.144$ (6) Å, $b = 10.017$ (2) Å, $c = 10.745$ (2) Å, $\alpha = 97.38$ (2)°, $V = 2577$ Å³, $R = 0.084$ for 2440 reflections having $I > 3\sigma(I)$.

Introduction

Heteroallenes have a potential for the formation of carbon-carbon bonds and, as far as carbon disulfide and isothiocyanate are concerned, for the elaboration of sulfur-containing inorganic and organic substrates. However, this requires activation of the heteroallene, which can be achieved by coordination to a metal center.¹⁻⁴ Examples of metal-promoted dimerization of heteroallenes involving

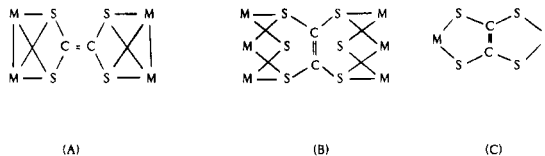
(1) Dixneuf, P. H.; Adams, R. D., Report of the International Seminar on the Activation of Carbon Dioxide and Related Heteroallenes on Metal Centers, Rennes, France, 1981.

(2) (a) Ibers, J. A. *Chem. Soc. Rev.* **1982**, II, 57. (b) Werner, H. *Coord. Chem. Rev.* **1982**, 43, 165 and references therein.

(3) Bianchini, C.; Mealli, C.; Meli, A.; Sabat, M. In *Stereochemistry of Organometallic and Inorganic Compounds*; Bernal, I., Ed.; Elsevier: Amsterdam, 1986, p 146.

(4) (a) Ngounda, M.; Le Bozec, H.; Dixneuf, P. H. *J. Org. Chem.* **1982**, 47, 4000. (b) Le Bozec, H.; Dixneuf, P. H. *J. Chem. Soc., Chem. Commun.* **1983**, 1462.

Scheme I

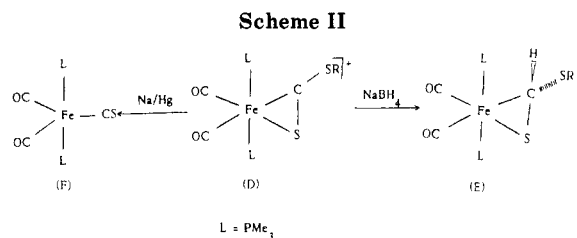


the formation of carbon-heteroatom bonds have been reported.⁵ These result from oxidative, "head-to-tail" coupling. Only a few processes involving "head-to-head" C-C bond coupling of heteroallenes have been discovered.⁶⁻¹²

(5) (a) Werner, H.; Kolb, O.; Feser, R.; Schubert, U. *J. Organomet. Chem.* **1980**, 191, 283. (b) Cowie, M.; Dwight, S. K. *J. Organomet. Chem.* **1981**, 214, 233. (c) Thewissen, D. H. M. W. *J. Organomet. Chem.* **1980**, 188, 211.

(6) Coucouvanis, D. *J. Am. Chem. Soc.* **1971**, 93, 1786.

(7) Pasquali, M.; Floriani, C.; Chiesi-Villa, A.; Guastini, C. *Inorg. Chem.* **1981**, 20, 349.



Early electrochemical studies⁶ of a bis(dithiooxalato)copper(II) system showed a reversible C–C bond formation between two sulfur-coordinated SCO ligands. C–C coupling of carbodiimide was observed by reaction with Cp₂Ti(CO)₂⁷ to give (Cp₂Ti)(RN)₂C–C(NR)₂(TiCp₂). C–C coupling of CS₂ was first achieved by reaction with Fe₃(CO)₁₂⁸ and afforded the complex (OC)₆Fe₂(S₂C–CS₂)–Fe₂(CO)₆ of type A, and ((C₅H₅)Ni)₂(CO)₂ and ((C₅Me₅)Ni)₂(CO)₂⁹ also react with CS₂ to give ((C₅H₅)Ni)₃(μ₂-S)₂(C₂S₄) of type B and ((C₅Me₅)Ni)₂(C₂S₄) of type C, respectively (Scheme I). The treatment of (triphos)MCl(CX₂) complexes (M = Rh, Ir; CX₂ = CSe₂,¹⁰ CS₂¹¹) with Lewis acids or even alcohols provide a general route to the formation of (triphos)M(C₂X₂)M(triphos)²⁺ cations of type C for which the dimerization has been rationalized.¹²

We wish to report a new type of C–C bond formation from a CS₂ derivative coordinated to an iron center. This reaction was found in the course of our initial effort to reduce alkylated Fe(η²-CS₂) derivatives, namely, Fe(η²-CS₂R)⁺ cations. This C–C coupling reaction involves a one-electron process, either from borohydride or from sodium amalgam, and leads to the dimerization of the η²-CS₂R group to afford tetrathiooxalate iron derivatives. The reaction pathways are based on the X-ray structure determination of two key derivatives of tetrathiooxalate, one coordinated to a binuclear and the other coordinated to a mononuclear iron moiety.

The reaction of L_nM(η²-CS₂R)⁺ cations with sodium borohydride has been shown to markedly depend on the nature of the L_nM moiety. The first reported example¹³ indicated that Os(η²-CS₂Me)(CO)₂(PPh₃)₂⁺ with NaBH₄ gave Os(H)(η¹-CS₂Me)(CO)₂(PPh₃)₂ which eventually, on heating, lost MeSH to afford the complex Os(CS)(CO)₂(PPh₃)₂. The complex [N(CH₂CH₂PPh₂)₃Co(η²-CS₂Me)⁺]¹⁴ under similar conditions led directly to elimination of the SMe group and formation of N(CH₂CH₂PPh₂)₃Co(CS)-BPh₄. By contrast, Cp₂(Bu)Nb(η²-CS₂Me)⁺ gave an unidentified adduct with borohydride which eventually transformed into Cp₂(Bu)Nb(η²-HCS₂Me).¹⁵ Recently we observed that [Fe(η²-CS₂Me)(CO)₂(L)₂⁺] (D, L = PMe₃) behaved toward NaBH₄ quite differently. Addition of hydride to the coordinated CS₂Me carbon took place affording the dithioformate iron complex E¹⁶ (Scheme II).

Conversely, reduction of D, containing PMe₃ groups, with sodium amalgam yielded the Fe⁰(CS) complex F. We now wish to show that the presence of PPh₃ groups in a complex of type D reorientates the course of the reactions with either borohydride or sodium amalgam.

Experimental Section

Syntheses. All reactions were carried out under a nitrogen atmosphere by using Schlenk techniques. NMR spectra were recorded on Bruker WP 80 FT (¹H, ³¹P, ¹³C) and on Bruker AM 300 WB FT (¹³C) instruments, and mass spectra were obtained with a Varian MAT 311 spectrometer at the "Centre de Mesures Physiques de l'Ouest", University of Rennes, Rennes, France. Elemental analyses were performed by CNRS, Villeurbanne, France.

Materials. Solvents were dried by reflux over appropriate drying agents and stored under inert atmosphere. Tetrahydrofuran and diethyl ether were distilled over sodium benzophenone ketyl, pentane, hexane, and acetonitrile were distilled over calcium hydride, and dichloromethane was distilled over phosphorus pentoxide first and then over calcium hydride.

Electrochemical Studies. Cyclic voltammetric measurements were obtained with the use of a conventional three-electrode system. The working electrode was a platinum electrode. A Tacussel UAP-4 or PAR Model 362 potentiostat and a Kipp and Zonen BD 90 X-Y recorder were used for cyclic voltammetric experiments. All the measurements were carried out at 25 °C under a nitrogen atmosphere with a solution of the complex (1.4–1.5 × 10⁻³ M) in 0.1 M Bu₄NPF₆/CH₃CN. All the potentials are referred to a saturated calomel electrode.

Synthesis of Cationic Complexes 2. Complexes 2a–c were prepared from Fe(η²-CS₂)(CO)₂(PPh₃)₂^{17,18} (1) in dichloromethane at room temperature with an excess of methyl iodide, ethyl iodide, or 2-methylallyl chloride according to the procedure published for 2a.^{17,18} The yellow salts 2a–c were thus obtained.

2a: 95% (810 mg); IR (Nujol) 2050, 1978 cm⁻¹. **2b:** 87% (755 mg); IR (Nujol) 2040, 1970 cm⁻¹. **2c:** 90% (760 mg); IR (Nujol) 2040, 1980 cm⁻¹.

Complex 2h was obtained from Fe(η²-CS₂)(CO)₂(P(OMe)₃)₂¹⁸ according to the general procedure.¹⁷

Complexes 2d and 2e were made by addition of HBF₄·OEt₂ (1.2 mmol, 0.3 mL) to the solution of Fe(η²-CS₂)(CO)₂(PPh₃)₂¹⁸ (1) (0.712 g, 1 mmol) in 20 mL of dichloromethane, followed by addition of 1.1 mmol of the unsaturated carbonyl compound, pulegone (**d**) or benzylideneacetone (**e**), in 5 mL of dichloromethane. The mixture was stirred at room temperature for 15 min. The solution was concentrated to ca. 5 mL, and then addition of diethyl ether led to the precipitation of the salt **2d** or **2e**.

2d: 80% (0.73 g) obtained from 1 mL of (+)-pulegone; mp 145–146 °C; IR (Nujol) 2045, 1980, 1700 cm⁻¹; ³¹P NMR (CDCl₃, 32.38 MHz, 305 K) δ 55.08 (s, PPh₃). Anal. Calcd for C₄₇H₄₃P₂O₃S₂FeBF₄: C, 61.78; H, 4.97; P, 6.50. Found: C, 61.56; H, 4.60; P, 7.02.

2e: 75% (0.69 g) obtained from 0.15 mL of 4-phenyl-3-buten-2-one; mp 163–165 °C; IR (Nujol) 2050, 1975, 1710 cm⁻¹; ³¹P NMR (CDCl₃, 32.38 MHz, 305 K) δ 50.92 (s, PPh₃). Anal. Calcd for C₄₉H₃₉P₂O₃S₂FeBF₄: C, 62.11; H, 4.47; P, 6.54. Found: C, 62.82; H, 4.82; P, 7.01.

Synthesis of Complexes 3. Method A (3a–c): Addition of Borohydride to Complexes 2. The addition of 2 equivalents of NaBH₄ (0.38 g) to a THF solution (100 mL) of **2a** (5 mmol, 4.27 g) at room temperature led after 2 h of stirring to the formation of a purple product. Solvent evaporation under reduced pressure and silica gel chromatography under nitrogen of the resulting mixture with ether and then THF as eluents gave 64% yield of the compound **3a** after recrystallization in THF/hexane. **3b** (55%) and **3c** (35%) were also obtained by using the same procedure from **2b** and **2c**.

Method B (3a–c): Reduction of Complexes 2 with Na/Hg. A THF (20 mL) solution of **2a** (0.5 mmol, 0.43 g) was added to

(8) Broadhurst, P. V.; Johnson, B. F. G.; Lewis, J.; Raithby, P. R. *J. Chem. Soc., Chem. Commun.* **1982**, 140.

(9) Maj, J. J.; Rae, A. D.; Dahl, L. F. *J. Am. Chem. Soc.* **1982**, *104*, 4278.

(10) Bianchini, C.; Mealli, C.; Meli, A.; Sabat, M. *J. Chem. Soc., Chem. Commun.* **1984**, 1647.

(11) Bianchini, C.; Mealli, C.; Meli, A.; Sabat, M. *Inorg. Chem.* **1984**, *23*, 4125.

(12) Bianchini, C.; Mealli, C.; Meli, A.; Sabat, M.; Zanella, P. *J. Am. Chem. Soc.* **1987**, *109*, 185.

(13) Collins, T. J.; Roper, W. R.; Town, K. G. *J. Organomet. Chem.* **1976**, *121*, C41.

(14) Bianchini, C.; Masi, D.; Mealli, C.; Meli, A.; Sabat, M.; Scapacci, G. *J. Organomet. Chem.* **1984**, *273*, 91.

(15) Amaudrut, J.; Sala-Pala, J.; Guerschais, J. E.; Mercier, R.; Douglade, J. *J. Organomet. Chem.* **1982**, *235*, 301.

(16) Touchard, D.; Dixneuf, P. H.; Adams, R. D.; Segmuller, B. E. *Organometallics* **1984**, *3*, 640.

(17) Touchard, D.; Le Bozec, H.; Dixneuf, P. H.; Carty, A. J. *Inorg. Chem.* **1981**, *20*, 1811.

(18) Le Bozec, H.; Dixneuf, P. H.; Carty, A. J.; Taylor, N. J. *Inorg. Chem.* **1978**, *17*, 2568.

5 mL of 1% sodium amalgam (1 mmol of Na) and stirred at room temperature. The reaction was monitored by using thin-layer chromatography. After 20 min, the reaction gave a mixture of two complexes, **3a** (purple) and **4a** (blue) that were separated by column chromatography (eluents, pentane-ether for **4a** (traces) and then THF for **3a** (major)). Crystallization in THF-hexane led to 40% yield of **3a**. Similarly **3b** (35%) and **3c** (30%) were obtained from **2b** and **2c**.

Method C (3d,e): Reduction with Magnesium. Activated magnesium (4 equiv) was prepared by stirring 4 mmol of Mg with 1 mmol of HgCl₂ in THF for 30 min, followed by decantation of the solution and washing of the magnesium with THF.¹⁹ Complex **2d** (915 mg, 1 mmol) or **2e** (920 mg, 1 mmol) in 20 mL of THF was added to the activated magnesium. The mixture was stirred at room temperature for 24 h. Filtration, solvent evaporation, and silica-gel chromatography under nitrogen (eluent, hexane-ether) led to 35% of **3d** (210 mg) and 30% of **3e** (180 mg).

Characterization of Complexes 3. **3a:** mp 176–178 °C; IR (Nujol) 1910 (vs), 1950 (s), 1930 (vs), 1910 (m) cm⁻¹; ³¹P NMR (CD₂Cl₂, 309 K, 32.38 MHz) δ 58.4 (s, PPh₃); ¹H NMR (CD₂Cl₂, 305 K, 80 MHz) δ 7.70, 7.42 (m, C₆H₅), 1.61 (s, SMe). Anal. Calcd for C₂₂H₁₈O₂PS₂Fe: C, 56.78; H, 3.89; P, 6.65; S, 13.78. Found: C, 56.50; H, 3.75; P, 6.36; S, 13.40.

3b: mp 120–122 °C; IR (Nujol) 2000 (vs), 1975 (vs), 1958 (s), 1935 (m) cm⁻¹; ³¹P NMR (C₆D₆, 306 K, 32.38 MHz) δ 58.8 (s, PPh₃); ¹H NMR (C₆D₆, 300 K, 80 MHz) δ 7.8 (m, C₆H₅), 2.30 (q, CH₂, ³J = 7.1 Hz), 0.90 (t, CH₃). Anal. Calcd for C₂₃H₂₀O₂PS₂Fe: C, 57.63; H, 4.20; P, 6.46; S, 13.38. Found: C, 57.52; H, 4.78; P, 6.48; S, 13.43.

3c: mp 126–127 °C; IR (Nujol) 1990 (s), 1940 (s), 1910 (s), 1905 (m) cm⁻¹; ³¹P NMR (C₆D₆, 300 K, 32.38 MHz) δ 81.18 (s, PPh₃); ¹H NMR (C₆D₆, 300 K, 80 MHz) δ 7.68, 7.39 (m, C₆H₅), 4.70 (s, =CH₂), 2.81 (s, CH₂), 1.60 (s, =CH₃). Anal. Calcd for C₂₄H₂₂O₂PS₂Fe: C, 58.49; H, 4.46; P, 6.28. Found: C, 58.30; H, 4.42; P, 6.30.

3d: mp 147–150 °C; IR (Nujol) 1985 (s), 1950 (vs), 1920 (s), 1885 (m), 1720 (m) cm⁻¹; ³¹P NMR (CDCl₃, 304 K, 32.38 MHz) δ 63.02 (s, PPh₃). Anal. Calcd for C₃₁H₃₂O₃PS₂Fe: C, 61.69; H, 5.34; S, 10.62; P, 5.13. Found: C, 61.90; H, 5.48; S, 10.68; P, 5.17.

3e: mp 156–158 °C; IR (Nujol) 1990 (s), 1950 (vs), 1915 (s), 1890 (m), 1720 (m) cm⁻¹; ³¹P NMR (CDCl₃, 304 K, 32.38 MHz) δ 63.32 (s, PPh₃). Anal. Calcd for C₃₁H₂₆O₃PS₂Fe: C, 62.32; H, 4.39; S, 10.73; P, 5.18. Found: C, 62.09; H, 4.58; S, 10.34; P, 5.25.

Synthesis of Complexes 4. Method A (4a–e): Oxidation of 3. The isolated complexes **3** in THF solution were transformed slowly into the products **4** in the presence of air. This transformation was accelerated by addition of acids or ceric salts. For example, 1 mmol (0.87 g) of **3a** in THF (20 mL), stirred for 1 h with an excess of Ce⁴⁺ salt (Ce(NO₃)₄) and in the presence of air, gave a blue solution. Filtration, evaporation of the solvent under reduced pressure and silica gel chromatography under nitrogen of the resulting mixture with pentane gave, after crystallization in pentane, a 30% yield of **4a**. The same complex **4a** was obtained in similar yield, but after 10 min at room temperature, when two drops of (14 M) HNO₃ were added to the solution of **3a** in the presence of air. **4b** (30%), **4c** (35%), **4d** (10%), and **4e** (5%) were obtained analogously.

Method B (4a–c): Reduction of 2. Complex **2a** (0.5 mmol, 0.43 g) in 20 mL of THF was added to 5 mL of 1% sodium amalgam. The reaction solution rapidly turned purple and then blue. After 1.5 h of stirring at room temperature only complex **4a** (blue) was present, as indicated by thin-layer chromatography (eluent, pentane). Silica gel chromatography (pentane) gave 40% yield of blue crystals of **4a**. Similarly **4b** and **4c** were obtained in 30% and 25% yields, respectively, from **2b** (0.41 g) and **2c** (0.40 g).

Characterization of Complexes 4. **4a:** mp 130–131 °C; IR (Nujol) 2010 (vs), 1950 (vs), 1100 (vs) cm⁻¹; ³¹P NMR (CDCl₃, 309 K, 32.38 MHz) δ 43.35 (s, PPh₃); ¹H NMR (CDCl₃, 305 K, 80 MHz) δ 7.66 (m, C₆H₅), 1.55 (s, SMe). Anal. Calcd for C₂₄H₂₁O₂PS₄Fe: C, 51.80; H, 3.80; P, 5.56; S, 23.04. Found: C, 52.11; H, 3.83; P, 5.97; S, 22.29.

4b: mp 168–170 °C; IR (Nujol) 2005 (vs), 1950 (vs) cm⁻¹; ³¹P NMR (C₆D₆, 308 K, 32.38 MHz) δ 41.6 (s, PPh₃); ¹H NMR (C₆D₆, 306 K, 80 MHz) δ 7.7 (m, C₆H₅), 2.20 (q, CH₂, ³J = 7.0 Hz), 0.80 (t, CH₃, ³J = 7.0 Hz). Anal. Calcd for C₂₅H₂₅O₂PS₄Fe: C, 53.42; H, 4.31; S, 21.94. Found: C, 53.15; H, 4.34; S, 21.24.

4c: mp 168–170 °C; IR (Nujol) 2000 (vs), 1930 (vs), 1080 (vs) cm⁻¹; ³¹P NMR (C₆D₆, 306 K, 32.28 MHz) δ 64.86 (s, PPh₃); ¹H NMR (C₆D₆, 306 K, 80 MHz) δ 6.98 (m, C₆H₅), 4.81 and 4.67 (s, =CH₂), 3.77 (s, SCH₂), 1.79 (s, CH₃). Anal. Calcd for C₃₀H₃₁O₂PS₄Fe: C, 56.22; H, 4.81; P, 4.88. Found: C, 56.25; H, 4.67; P, 5.02.

4d: IR (Nujol) 1995 (vs), 1945 (vs), 1720 (m) cm⁻¹. Anal. Calcd for C₄₂H₄₉O₄PS₄Fe: C, 60.56; H, 5.93. Found: C, 59.88; H, 6.08.

4e: IR (Nujol) 1990 (vs), 1945 (vs), 1680 (m) cm⁻¹.

Reductions of Cation 2h. Reduction with NaBH₄. **Synthesis of 5–7.** The addition of 2 equiv of NaBH₄ (0.152 g) to a THF solution (40 mL) of **2h** (2 mmol, 1.2 g) led after 3 h of stirring at room temperature to the formation of two different products. Solvent evaporation under reduced pressure and silica gel chromatography under nitrogen of the resulting mixture gave the unstable yellow complex **5** (eluent, pentane) and then the red oily complex **6** (eluent, ether) in 30% yield.

After its extraction in pentane, the very unstable intermediate **5** was solubilized in benzene. To this solution was added an excess of dimethyl acetylenedicarboxylate immediately. The solution color turned rapidly from yellow to red. After 30 min of reaction at room temperature, thick-layer chromatography (eluent, ether) followed by crystallization in ether led to 0.12 g of red crystals of **7** (10%).

Characterization of Complexes 6 and 7. **6:** IR (Nujol) 1995 (vs), 1950 (m), 1930 (vs), 1920 (m) cm⁻¹; ³¹P NMR (C₆D₅CD₃, 309 K, 32.38 MHz) δ 275.5 (s, P(OMe)₃); ¹H NMR (C₆D₅CD₃, 309 K, 80 MHz) δ 2.1 (s, SMe), 3.5 (d, P(OMe)₃, J_{PH} = 11.5 Hz); mass spectrum, *m/e* found 625.8493 (calcd for (M - CO)⁺ (C₁₃H₂₄O₉-P₂S₄Fe₂), 625.8477). **7:** mp 162 °C dec; IR (Nujol) 1965 (vs), 1690 (s), 1720 (s), 1590 (m) cm⁻¹; mass spectrum, *m/e* found 593.9805 (calcd for M⁺ (C₁₆H₂₂O₁₂P₂S₂Fe), 593.9846); ¹H NMR (CDCl₃, 303 K, 80 MHz) δ 3.79 and 3.69 (dd, P(OMe)₃, ³J_{PH} = 11 Hz), 3.77 and 3.72 (s, CO₂Me), 2.08 and 2.04 (SMe), CH masked by CO₂Me and P(OMe)₃.

Reduction with Activated Magnesium: Synthesis of 6. Complex **2h** (1 mmol, 0.6 g) in THF solution (20 mL) was added to 4 equiv of magnesium activated by HgCl₂.¹⁹ The mixture was stirred at room temperature for 12 h. The solution turned red, and after filtration, solvent evaporation, and silica gel column chromatography under nitrogen (eluent, hexane-ether) we obtained a 30% yield of **6** (0.18 g).

Reduction with Sodium Amalgam: Synthesis of 8 and 9. A THF (20 mL) solution of **2h** (1 mmol, 0.6 g) was added to 5 mL of 1% sodium amalgam and the mixture stirred at room temperature. After 2 h, the solution turned violet and thin-layer chromatography showed the formation of two products: yellow and violet. The two complexes were separated by silica gel chromatography under nitrogen (eluent, pentane-ether) and obtained in 5% (**8**, yellow) and 35% (**9**, violet) yields.

Characterization of Complexes 8 and 9. **8:** IR (Nujol) 1970 (vs), 1910 (vs), 1240 (vs) cm⁻¹; mass spectrum, *m/e* found 403.9538 (calcd for M⁺ (C₉H₁₈O₈P₂SFe), 403.9538), 367 (M - CO⁺), 348 ((M - 2CO)⁺); ¹H NMR (C₆D₆, 306 K, 80 MHz) δ 3.67 (t, P(OMe)₃, J_{PH} = 12 Hz).

9: IR (Nujol) 1955 (vs) cm⁻¹; mass spectrum, *m/e* found 513.9247 (calcd for M⁺ (C₁₁H₂₄O₇P₂S₄Fe), 513.9229), 486 (M - CO⁺); ¹H NMR (C₆D₅CD₃, 306 K, 80 MHz) δ 3.24 (t, P(OMe)₃, [³J_{PH} + ⁵J_{PH}] = 12.2 Hz); ³¹P NMR (C₆D₅CD₃, 306 K, 32.38 MHz) δ 173.6 (s, P(OMe)₃).

X-ray Diffraction Studies. A summary of crystal data for both compounds **3a** and **4a** is reported in Table I. Details of the data collection and crystal structure solution are given below, separately.

Complex 3a. The sample was studied with an automatic CAD-4 Enraf-Nonius diffractometer. The parameters of the unit cell were determined and refined with a set of 25 reflections (6° < θ < 13°). During the data collection (Table I), three orientation reflections (measured each 400 data without reorientation) and three standard reflections (measured each 3600 s without appreciable decay) were considered. The data were corrected for

(19) Sikora, D. J.; Rausch, M. D.; Rogers, R. D.; Atwood, J. L. *J. Am. Chem. Soc.* **1981**, *103*, 1265.

Table I. Summary of Crystal Data

	3a	4a
formula	C ₄₄ H ₃₆ O ₄ P ₂ S ₄ Fe ₂	C ₂₄ H ₂₁ O ₂ PS ₄ Fe
mol wt	930.7	556.5
cryst size, mm	0.10 × 0.15 × 0.2	0.425 × 0.15 × 0.20
system	triclinic	monoclinic
space group	<i>P</i> $\bar{1}$	<i>P</i> 2 ₁ / <i>a</i>
<i>a</i> , Å	9.669 (2)	24.144 (6)
<i>b</i> , Å	13.477 (3)	10.017 (2)
<i>c</i> , Å	17.323 (3)	10.745 (2)
α , deg	101.1 (2)	90.0
β , deg	91.5 (2)	97.38 (2)
γ , deg	110.3 (2)	90.0
<i>V</i> , Å ³	2048	2577
<i>Z</i>	2	4
<i>d</i> _{calcd} , g·cm ⁻³	1.51	1.43
μ (Mo K α), cm ⁻¹	10.13	9.75
radiation	graphite-monochromated Mo K α ($\lambda = 0.71069$ Å)	
2 θ range, deg	2–50	5–50
scan width, $\omega/2\theta$	1.00	1.00
scan speed, deg·s ⁻¹	<i>t</i> _{max} = 60 s	0.05
octants collected	<i>h</i> , $\pm k$, $\pm l$	$\pm h$, <i>k</i> , <i>l</i>
total data	7220	5057
unique data (<i>I</i> > 3 σ (<i>I</i>))	3802 (<i>I</i> > σ (<i>I</i>))	2400 (<i>I</i> > 3 σ (<i>I</i>))
<i>R</i>	0.058	0.084
<i>R</i> _w	0.058	0.095

Lorentz and polarization effects with a small linear absorption coefficient (μ (Mo K α) = 10.13 cm⁻¹), and equidimensional crystal corrections for absorption were deemed unnecessary. Anomalous dispersion corrections were taken from ref 20. The structure was solved with a Patterson map and several Fourier differences. After isotropic and anisotropic refinements of Fe, S, P, C, and O atoms, many hydrogen atoms were located with a Fourier difference map. The remaining ones were set in calculated positions. The full-matrix least-squares refinement (*x*, *y*, *z*, and β_{ij} for non-hydrogen atoms; *x*, *y*, and *z* for hydrogen atoms) gave $R = \sum ||F_o| - |F_c|| / |F_o| = 0.058$ and $R_w = [\sum w(|F_o| - |F_c|)^2 / \sum w|F_o|^2]^{1/2} = 0.058$. The final residual electronic density is less than 0.7 e Å⁻³. Final coordinates of all the non-hydrogen atoms are given in Table II.

Complex 4a. A Philips PW 1100 automated four-circle diffractometer was used for experimental work under Mo K α radiation. A set of high-angle reflections was used for the centering procedure of the crystal. Three standard reflections were collected every 2 h (no appreciable decay of intensity was observed). The data were corrected for Lorentz and polarization effects. Numerical absorption corrections were applied with transmission factors ranging between 0.87 and 0.72. Atomic scattering factors were those tabulated by Cromer and Weber.²¹ Anomalous dispersion corrections were taken from ref 20. Anomalous dispersion corrections were taken from ref 20. The computational work was essentially performed by using the SHELX76 system.²² The structure was solved by direct methods and Fourier techniques. Rigid-body models (*D*_{6h} symmetry) for the phenyl rings were adopted during the least-squares refinement. The hydrogen atoms were introduced at calculated positions (C–H = 1.0 Å). Anisotropic thermal parameters were used for Fe, P, and S atoms. The final difference Fourier map is essentially featureless with largest peaks less than 1 e/Å³. Final coordinates of all the non-hydrogen atoms are reported in Table III.

Results and Discussion

Synthesis and Characterization of Complexes 3.

The reaction of the Fe(η^2 -CS₂R)⁺I⁻ complex **2a** with 2 equiv of NaBH₄ in THF at room temperature for 3 h led to the gradual formation of a purple derivative, **3a**, which was obtained, after purification by chromatography, in 64% yield. Similarly, the salt **2b** gave the compound **3b**

(20) *International Tables for Crystallography*; Kynoch: Birmingham, 1974; Vol. 4.

(21) Cromer, D. T.; Weber, J. T. *Acta Crystallogr.* 1965, 18, 104.

(22) Sheldrick, G. M. SHELX76, Program for Crystal Structure Determinations; University of Cambridge: Cambridge, 1976.

Scheme III

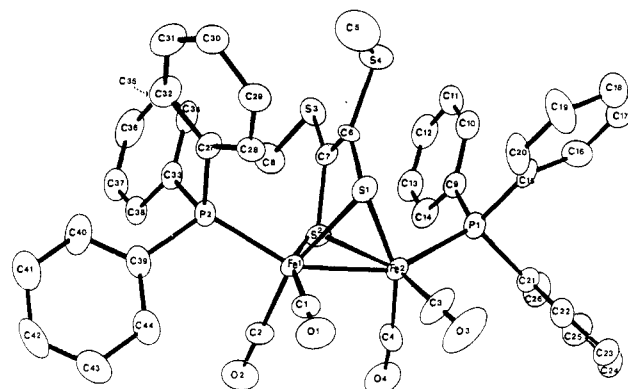
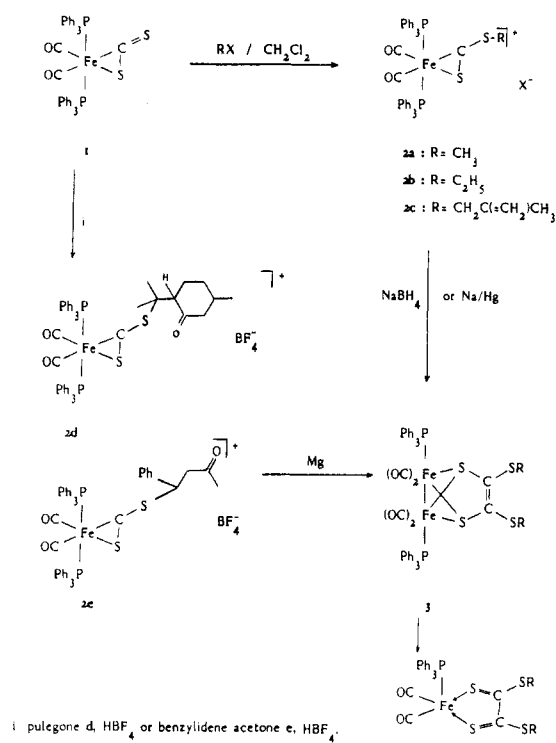


Figure 1. ORTEP drawing of Fe₂S₂C₂(SMe)₂(CO)₄(PPh₃)₂ (**3a**).

(55%), which, like **3a**, is air-sensitive in solution. Complex **3a** was also obtained in similar yield (62–65%) by reaction of **2a** with 2 equiv of (Ph₃PNPPh₃)BH₄ or by reaction of NaBH₄ with **2a** containing the noncoordinating anion X⁻ = PF₆⁻ (Scheme III).

Complexes **3a** and **3b** showed four terminal carbonyl absorption bands in the infrared spectrum and contained, as indicated by ¹H NMR, one SR group per PPh₃ ligand. The X-ray diffraction structure of **3a** was determined. It establishes (Figure 1) that complexes **3** are Fe–Fe bimetallic derivatives with a dialkyl tetrathiooxalate ligand bridging two Fe(CO)₂(PPh₃) moieties. Thus the formation of complexes **3**, formally resulting from C–C and Fe–Fe bond couplings, requires an overall two-electron reduction of two **2a** molecules and elimination of one PPh₃ group from each iron center.

It is worth recalling that in the formation of Fe(η^2 -CH(SMe)S)(CO)₂(PMe₃)₂ from Fe(η^2 -CS₂Me)(CO)₂(PMe₃)₂⁺ the function of borohydride was to release the hydride that was incorporated in the former complex.¹⁶ Conversely, the formation of **3** requires one-electron transfer from borohydride to complexes **2**, without incorporation of hydride. This observation suggested that complexes **3** could be also obtained by a one-electron reduction, with the appropriate

Table II. Positional Parameters and Their Estimated Standard Deviations for $\text{Fe}_2\text{S}_2\text{C}_2(\text{SMe})_2(\text{CO})_4(\text{PPh}_3)_2$ (**3a**)^a

atom	x	y	z	U, Å ²	atom	x	y	z	U, Å ²
Fe(1)	0.4955 (1)	0.39470 (8)	0.20368 (7)	1.54 (2)	C(35)	0.654 (1)	0.1745 (6)	0.3902 (5)	2.9 (2)
Fe(2)	0.4875 (1)	0.58040 (8)	0.24957 (7)	1.59 (2)	C(36)	0.796 (1)	0.2350 (6)	0.4229 (5)	3.2 (2)
S(1)	0.6805 (2)	0.5472 (1)	0.1920 (1)	1.58 (4)	C(37)	0.8843 (9)	0.3084 (6)	0.3836 (5)	2.9 (2)
S(2)	0.5517 (2)	0.4854 (1)	0.3325 (1)	1.74 (4)	C(38)	0.8314 (9)	0.3220 (6)	0.3136 (5)	2.3 (2)
S(3)	0.8558 (2)	0.5731 (2)	0.4317 (1)	2.45 (5)	C(39)	0.5009 (9)	0.1360 (6)	0.1373 (5)	2.2 (2)
S(4)	0.9898 (2)	0.6625 (2)	0.2802 (1)	2.60 (5)	C(40)	0.3587 (9)	0.1075 (6)	0.1015 (5)	2.8 (2)
P(1)	0.5903 (2)	0.7562 (2)	0.3115 (1)	1.80 (5)	C(41)	0.276 (1)	0.0028 (7)	0.0616 (6)	3.8 (3)
P(2)	0.6125 (2)	0.2751 (2)	0.1873 (1)	1.62 (4)	C(42)	0.336 (1)	-0.0760 (7)	0.0582 (6)	4.1 (3)
O(1)	1.3721 (6)	0.3580 (5)	0.0410 (3)	3.68 (2)	C(43)	0.478 (1)	-0.0504 (6)	0.0928 (6)	3.4 (2)
O(2)	0.2153 (6)	0.2589 (5)	0.2486 (4)	3.76 (2)	C(44)	0.5585 (9)	0.0519 (6)	0.1330 (5)	2.6 (2)
O(3)	0.3767 (7)	0.6126 (5)	0.1029 (4)	4.8 (2)	H(10)	0.889 (7)	0.859 (5)	0.390 (4)	3.2*
O(4)	0.2005 (6)	0.5182 (5)	0.3122 (4)	4.72 (2)	H(11)	0.977 (8)	0.909 (5)	0.531 (4)	3.2*
C(1)	0.4214 (8)	0.3712 (6)	0.1049 (5)	2.24 (2)	H(12)	0.866 (7)	0.825 (5)	0.622 (4)	3.2*
C(2)	0.3273 (8)	0.3124 (6)	0.2304 (4)	1.84 (4)	H(13)	0.615 (7)	0.709 (5)	-0.572 (4)	3.2*
C(3)	0.4195 (8)	0.6021 (7)	0.1629 (5)	2.88 (2)	H(14)	0.495 (7)	0.685 (5)	0.444 (4)	3.2*
C(4)	0.3137 (9)	0.5474 (6)	0.2877 (5)	2.56 (2)	H(16)	0.730 (7)	0.735 (5)	0.158 (4)	3.2*
C(5)	1.041 (1)	0.6143 (8)	0.1866 (6)	3.84 (3)	H(17)	0.909 (7)	0.870 (5)	0.119 (4)	3.2*
C(6)	0.8078 (7)	0.5773 (5)	0.2788 (4)	1.52 (2)	H(18)	1.000 (7)	1.036 (5)	0.165 (4)	3.2*
C(7)	0.7505 (7)	0.5448 (5)	0.3408 (4)	1.52 (2)	H(19)	0.914 (7)	1.102 (5)	0.289 (4)	3.2*
C(8)	0.732 (1)	0.4864 (7)	0.4856 (5)	3.1 (2)	H(20)	0.742 (7)	0.984 (5)	0.348 (4)	3.2*
C(9)	0.6832 (8)	0.7805 (5)	0.4102 (5)	1.8 (2)	H(22)	0.401 (7)	0.792 (5)	0.209 (4)	3.2*
C(10)	0.8343 (8)	0.8452 (6)	0.4332 (5)	2.3 (2)	H(23)	0.252 (7)	0.893 (5)	0.237 (4)	3.2*
C(11)	0.8948 (9)	0.8566 (6)	0.5075 (5)	2.9 (2)	H(24)	0.209 (7)	0.997 (5)	0.361 (4)	3.2*
C(12)	0.814 (1)	0.8109 (6)	0.5625 (5)	3.0 (2)	H(25)	0.321 (7)	0.960 (5)	0.460 (4)	3.2*
C(13)	0.6665 (9)	0.7458 (6)	0.5409 (5)	2.7 (2)	H(26)	0.474 (7)	0.870 (5)	0.449 (4)	3.2*
C(14)	0.6017 (8)	0.7296 (6)	0.4654 (5)	2.3 (2)	H(28)	0.862 (7)	0.213 (5)	0.178 (4)	3.2*
C(15)	0.7258 (8)	0.8509 (5)	0.2628 (5)	1.9 (2)	H(29)	1.065 (7)	0.272 (5)	0.089 (4)	3.2*
C(16)	0.774 (1)	0.8165 (6)	0.1927 (6)	3.3 (2)	H(30)	1.076 (7)	0.360 (5)	-0.006 (4)	3.2*
C(17)	0.879 (1)	0.8895 (7)	0.1571 (6)	4.9 (3)	H(31)	0.887 (7)	0.417 (5)	-0.023 (4)	3.2*
C(18)	0.926 (1)	0.9969 (7)	0.1920 (6)	4.5 (3)	H(32)	0.695 (8)	0.381 (5)	0.057 (4)	3.2*
C(19)	0.8810 (9)	1.0336 (6)	0.2606 (6)	3.1 (2)	H(34)	0.507 (7)	0.138 (5)	0.296 (4)	3.2*
C(20)	0.7775 (8)	0.9605 (6)	0.2956 (5)	2.2 (2)	H(35)	0.592 (7)	0.116 (5)	0.407 (4)	3.2*
C(21)	0.4578 (7)	0.8280 (5)	0.3289 (5)	1.8 (2)	H(36)	0.821 (7)	0.221 (5)	0.463 (4)	3.2*
C(22)	0.3894 (8)	0.8410 (6)	0.2624 (5)	2.2 (2)	H(37)	0.969 (7)	0.351 (5)	0.408 (4)	3.2*
C(23)	0.2937 (9)	0.8988 (7)	0.2719 (6)	3.1 (2)	H(38)	0.894 (7)	0.379 (5)	0.291 (4)	3.2*
C(24)	0.2564 (9)	0.9359 (6)	0.3438 (6)	3.1 (2)	H(40)	0.324 (7)	0.167 (5)	0.100 (4)	3.2*
C(25)	0.322 (1)	0.9232 (7)	0.4091 (6)	3.5 (2)	H(41)	0.190 (7)	-0.001 (5)	0.030 (4)	3.2*
C(26)	0.4244 (9)	0.8686 (7)	0.4013 (5)	3.3 (2)	H(42)	0.298 (7)	-0.134 (5)	0.029 (4)	3.2*
C(27)	0.7707 (7)	0.3028 (5)	0.1264 (4)	1.5 (2)	H(43)	0.525 (7)	-0.100 (5)	0.093 (4)	3.2*
C(28)	0.8870 (8)	0.2643 (6)	0.1354 (5)	2.4 (2)	H(44)	0.653 (7)	0.070 (5)	0.168 (4)	3.2*
C(29)	0.9994 (8)	0.2867 (7)	0.0871 (5)	3.4 (2)	H(5A)	1.116 (7)	0.673 (5)	0.181 (4)	3.2*
C(30)	0.9981 (9)	0.3376 (7)	0.0272 (5)	2.7 (2)	H(5B)	1.018 (7)	0.540 (5)	0.179 (4)	3.2*
C(31)	0.8813 (9)	0.3728 (6)	0.0169 (5)	2.3 (2)	H(5C)	0.967 (7)	0.609 (5)	0.147 (4)	3.2*
C(32)	0.7689 (7)	0.3538 (6)	0.0656 (4)	1.8 (2)	H(8A)	0.764 (7)	0.484 (5)	0.527 (4)	3.2*
C(33)	0.6894 (8)	0.2582 (5)	0.2794 (4)	1.8 (2)	H(8B)	0.645 (7)	0.526 (5)	0.512 (4)	3.2*
C(34)	0.6001 (8)	0.1850 (6)	0.3187 (5)	2.0 (2)	H(8C)	0.712 (7)	0.419 (5)	0.463 (4)	3.2*

^a Parameters with an asterisk were refined isotropically. Anisotropically refined atoms are given in the form of the isotropic equivalent thermal parameter defined as $(1/3)[a^2B(1,1) + b^2B(2,2) + c^2B(3,3) + ab(\cos \gamma)B(1,2) + ac(\cos \beta)B(1,3) + bc(\cos \alpha)B(2,3)]$.

reducing reagent. Complex **2a** was therefore reacted in THF at room temperature with an excess of 1% sodium amalgam. A color change occurred rapidly, and monitoring of the reaction, using thin-layer chromatography, showed the formation of **3a** and a small amount of a blue product (**4a**) which increased with reaction time. After a short time, 20 min, column chromatography allowed successive isolation of traces of **4a** (eluent, pentane-ether) and then 40% of **3a** (eluent, THF). Analogously, **3b** was obtained in 35% yield by reduction of **2b** with sodium amalgam.

Complex **2c** containing an allyl group at the exocyclic sulfur atom was made in order to explore the possible involvement of the C=C double bond in the reaction. Complex **2c** in THF with NaBH_4 led to the formation of complex **3c** in 30% yield. Sodium amalgam also transformed **2c** into **3c**, which was isolated in (30%) after a 15 min reaction. It thus appeared that the presence of an allyl group did not modify the reactivity of complexes **2**. Consequently, the reactivity of complexes **2** with borohydride or a source of electrons was expected to be mainly determined by the potential of reduction of the iron cation **2**.

Complexes **2** were then studied by using cyclic voltammetry. In acetonitrile with $(\text{Bu}_4\text{N})\text{PF}_6$ as electrolyte, all

complexes showed a similar behavior: one irreversible reduction wave at negative potential was observed at a scan rate of $200 \text{ mV}\cdot\text{s}^{-1}$ (Table IV). Only for **2g** ($\text{L} = \text{PMe}_3$), with a higher scan rate, was a reversible wave observed. The reduction potential does not depend on the nature of the anion X^- (I^- , PF_6^-) for **2a**. By contrast, it depends strongly on the nature of both the phosphine and the R groups. The easiest reduction eventually leading to complexes **3** occurs with complexes **2a-c**, containing PPh_3 groups. For complexes **2f** and **2g**, containing more electron-donating phosphines, PMe_2Ph and PMe_3 , respectively, the reduction occurs at more negative potentials. These latter complexes when treated with borohydride do not capture an electron but give instead $\text{Fe}(\eta^2\text{-CH}(\text{SMe})\text{S})(\text{CO})_2(\text{PR}_3)_2$ complexes, via hydride addition to the CS_2R carbon.¹⁶ The large difference between the potential of borohydride (E° is -2.25 V vs SCE for the $1/2 \text{ H}_2/\text{H}^-$ system) and that of complexes **2a-c** (in the range -0.74 to -0.79 V vs SCE, Table IV) may be responsible for electron transfer, as opposed to hydride addition, to **2a-c**. The reduction of **2f** and **2g** requires an even stronger reducing reagent than hydride such as sodium amalgam. The nature of the PR_3 ligands is also critical in determining the reactivity pattern. In the formation of the $\text{Fe}(\text{CS})$ -

Table III. Final Atomic Coordinates and Thermal Parameters for $\text{FeS}_2\text{C}_2(\text{SMe})_2(\text{CO})_2(\text{PPh}_3)$ (4a)^a

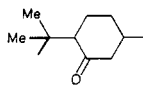
atom	x	y	z	$U_{\text{equiv}}^a \text{ \AA}^2$
Fe	1016 (1)	1669 (1)	1651 (1)	36 (1)
S(1)	1609 (1)	1112 (3)	3249 (2)	44 (1)
S(2)	1584 (1)	764 (3)	449 (3)	65 (2)
S(3)	2619 (1)	-672 (5)	3756 (4)	89 (2)
S(4)	2578 (2)	-1110 (4)	862 (4)	86 (2)
P(1)	562 (1)	2919 (2)	2927 (2)	32 (1)
O(1)	645 (5)	3499 (10)	-445 (9)	99 (7)
O(2)	136 (4)	-324 (9)	1325 (8)	77 (6)
C(1)	790 (4)	2767 (11)	375 (10)	51 (7)
C(2)	471 (5)	466 (11)	1445 (9)	51 (7)
C(3)	2105 (4)	130 (10)	2722 (10)	47 (6)
C(4)	2088 (4)	-38 (11)	1434 (11)	55 (7)
C(5)	2298 (7)	-821 (20)	5158 (16)	110 (14)
C(6)	2492 (9)	-702 (21)	-803 (17)	137 (16)
C21	599 (3)	1107 (5)	4890 (5)	49 (3)
C31	737 (3)	655 (5)	6118 (5)	60 (3)
C41	977 (3)	1528 (5)	7047 (5)	67 (3)
C51	1078 (3)	2853 (5)	6747 (5)	61 (3)
C61	940 (3)	3305 (5)	5518 (5)	46 (2)
C11	701 (3)	2432 (5)	4589 (5)	29 (2)
C22	-512 (3)	3127 (7)	3619 (5)	53 (3)
C32	-1093 (3)	3205 (7)	3385 (5)	66 (3)
C42	-1361 (3)	3105 (7)	2158 (5)	82 (4)
C52	-1047 (3)	2929 (7)	1166 (5)	100 (5)
C62	-466 (3)	2852 (7)	1401 (5)	64 (3)
C12	-199 (3)	2951 (7)	2628 (5)	38 (2)
C23	362 (2)	5700 (6)	2906 (7)	55 (3)
C33	526 (2)	7032 (6)	2858 (7)	64 (3)
C43	1085 (2)	7349 (6)	2796 (7)	60 (3)
C53	1479 (2)	6333 (6)	2782 (7)	67 (3)
C63	1315 (2)	5001 (6)	2829 (7)	57 (3)
C13	757 (2)	4684 (6)	2891 (7)	36 (2)

^a Atoms Fe through C₆, refined anisotropically, are given as U_{equiv} , remaining atoms were refined isotropically. Coordinates multiplied by 10⁴ and temperature factors by 10³.

(CO)₂(PMe₂R)₂ complexes, by Na/Hg reduction of Fe-(η^2 -CS₂R)(CO)₂(PMe₂R)₂⁺ cations, there was no elimination of PR₃ groups.²³ Thus, the lability of the Fe-PPh₃ bond in the reduced complexes 2a-c probably determined their transformation into 3a-c rather than into Fe⁰(CS)(CO)₂(PR₃)₂ complexes.

We have shown previously that complexes of type 2d and 2e, with structures similar to those of 2a-c, could be obtained easily.²⁴ Addition of an α,β -unsaturated ketone such as pulegone (**d**) and benzylideneacetone (**e**) to complex 1, in the presence of a slight excess of 1 equiv of HBF₄, afforded the red salts 2d (80%) and 2e (75%). These salts resulted from two-fragment addition, the uncoordinated and nucleophilic sulfur atom of 1 at the β -carbon and the proton at the α -carbon of the enone substrate. However, in the presence of a base, complexes 2d and 2e afforded immediately the precursor 1 and the enone. The addition of NaBH₄ to complexes 2d,e also led to their deprotonation and the release of complex 1 rather than formation of complexes 3d,e. Sodium amalgam could not be used to avoid the reduction of the ketone carbonyl. A milder reducing reagent had to be found to produce 3d and 3e. Cyclic voltammetry of 2d in acetonitrile indicated that the reduction potential ($E_c = -0.98$ V vs SCE) was much more negative than those of complexes 2a-c (Table IV). The R group bonded to the sulfur atom in 2d contains an electron-withdrawing carbonyl group. If its electronic influence was predominant, a shift toward a less negative value would have been expected. The observed shift may be due to the steric influence of the pulegone fragment that

Table IV. Reduction Potentials and Infrared Absorptions of Complexes $\text{Fe}(\eta^2\text{-CS}_2\text{R})(\text{CO})_2\text{L}_2^+\text{X}^-$ (2)

	L	-R	X ⁻	E_c^a , V	ν_{CO}^b
2a	PPh ₃	Me	I ⁻	-0.74	1978
					2050
2a	PPh ₃	Me	PF ₆ ⁻	-0.74	1978
					2050
2b	PPh ₃	Et	Br ⁻	-0.76	1975
					2050
2c	PPh ₃	CH ₂ C(Me)=CH ₂	Cl ⁻	-0.79	1980
					2040
2f	PMe ₂ Ph	Me	PF ₆ ⁻	-0.94	1970
					2040
2g	PMe ₃	Me	PF ₆ ⁻	-1.04	1965
					2035
2d	PPh ₃		BF ₄ ⁻	-0.98	1980
					2045
2h	P(OMe) ₃	Me	PF ₆ ⁻	-0.81	2020
					2075

^a Determined by cyclic voltammetry with a 1.5×10^{-3} M of complex in 0.1 M of Bu₄NPF₆ in CH₃CN (200 mV·s⁻¹). ^b In cm⁻¹ (Nujol mull).

probably creates an interaction with the PPh₃ groups. Consequently, a distortion in the structure of the molecule 2d, as compared to that of 2a-c, may be responsible for the observed shift. For a milder reagent able to reduce 2d we selected magnesium [$E^\circ(\text{Mg}^{2+}/\text{Mg}) = -2.62$ and $E^\circ(\text{Na}^+/\text{Na}) = -2.96$ V vs SCE]. When activated by treatment with mercury dichloride, magnesium slowly converted 2d and 2e into 3d and 3e. After 24 h at room temperature 3d and 3e were isolated in 35% and 30% yields, respectively. This simple reduction reaction allowed production of an iron complex of tetrathiooxalate containing two chiral ketone fragments in 3d.

Synthesis and Characterization of Complexes 4. During the isolation of 3a, it was observed that its solution in the presence of air turned from red to green. Thin-layer chromatography revealed the formation of a blue product. The formation of this blue compound, from a solution of 3a, was accelerated by the addition of several drops of an aqueous solution of either H₂O₂, nitric acid, or a ceric salt in the presence of air. When an aqueous solution of 3a was stirred with an aqueous solution of Ce(NO₃)₄ at room temperature in air atmosphere for 1 h, 3a was completely converted. Purification using chromatography and crystallization allowed the isolation of a 30% yield of the blue complex 4a. The same yield of 4a was obtained when a solution of HNO₃ was used. A similar transformation of 3b and 3c led to the isolation of the blue complexes 4b (30%) and 4c (35%) (Scheme III).

Complexes 4a-c showed in their infrared spectra two terminal carbonyl absorption bands. The ¹H NMR spectra indicated two SR groups per PR₃ ligand, suggesting the loss of a phosphorus ligand from 3. The ³¹P NMR spectra showed one single line at a slightly higher field for 4 than for 3.

Treatment of complexes 3d and 3e with a ceric salt also led to blue complexes but in low yield. 4d (10%) and 4e (5%) were only identified only on the basis of their infrared spectra that showed two terminal carbonyl absorptions, as in 4a-c, and one ketonic carbonyl absorption.

Formation of the same blue complexes 4 was observed when the reduction of the salts 2 with sodium amalgam was carried out for more than half an hour. The reaction of 4a in THF with sodium amalgam was complete after 1.5 h at 25 °C. Silica gel column chromatography allowed the isolation of 40% of 4a. 4b (30%) and 4c (25%) were obtained similarly by reduction of 3b and 3c for 1.5 h. The

(23) Touchard, D.; Lelay, C.; Fillaut, J.-L.; Dixneuf, P. H. *J. Chem. Soc., Chem. Commun.* 1986, 1, 37.

(24) Plusquellec, D.; Dixneuf, P. H. *Organometallics* 1982, 1, 1401.

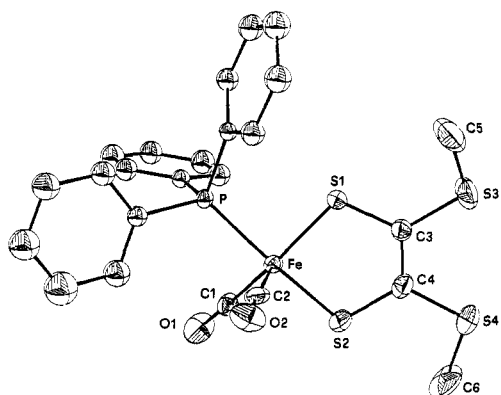


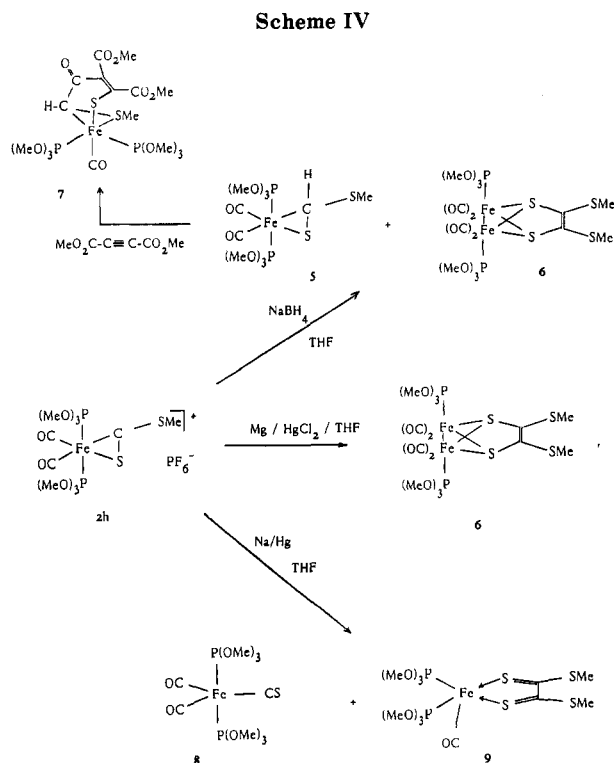
Figure 2. ORTEP drawing of $\text{FeS}_2\text{C}_2(\text{SMe})_2(\text{CO})_2(\text{PPh}_3)$ (**4a**).

direct reduction of the salts **2** presents the advantage of leading to either complexes **3** or **4** depending on the reaction time.

The structure of complexes **4** was based on an X-ray diffraction determination of **4a**. It shows (Figure 2) that the tetrathiooxalate ligand has been retained but its two thioketonic sulfur atoms are now bonded to one iron atom. Each iron atom retains one PPh_3 and two carbonyl ligands. Consequently, the overall transformation of **3** to **4** corresponds to the formal loss of one $\text{Fe}(\text{CO})_2(\text{PPh}_3)$ moiety, accompanied by a rearrangement of the coordinated tetrathiooxalate ligand.

Reactivity of the Derivative 2h, Containing P(OMe)₃ Groups. Cyclic voltammetry on the salt **2h**, containing $\text{P}(\text{OMe})_3$ groups, gave an E_c value of -0.81 V vs SCE. Whereas the electron-donating influence of L group ($\text{P}(\text{OMe})_3 < \text{PPh}_3 < \text{PMe}_2\text{Ph} < \text{PMe}_3$) is reflected in the $\nu(\text{CO})$ frequencies of complexes **2** (Table IV), the E_c value for **2h**, which lies between those of **2a** and **2f**, indicates that the electronic influence of the ligand L does not correlate with the reduction potential. The ease of reduction follows the sequence $\text{PPh}_3 > \text{P}(\text{OMe})_3 > \text{PMe}_2\text{Ph} > \text{PMe}_3$. This observation may be explained by the work of Giering et al.,²⁵ who interpreted unexpected values of potential in terms of steric effects. The more sterically encumbered complexes (e.g. **2a-c**) are easier to reduce than expected from consideration of the electronic effects of the ancillary ligands (e.g. than **2h**). The cathodic potential of **2h** between those of **2a** and **2f** led us to investigate whether its behavior toward hydride and reduction with magnesium or sodium amalgam were similar to that of **2a** or to that of **2f,g**.

Two equivalents of NaBH_4 were added to a THF solution of **2h**, and after 3 h at room temperature, a yellow and a red product were separated by using silica gel column chromatography and elution first with pentane and then with ether. From the ether fraction 30% yield of complex **6** was isolated. An analogous structure to that of **3** was established for **6** on the basis of a mass spectrum and other spectroscopic data (Scheme IV). The first fraction from chromatography eluted with pentane afforded an unstable intermediate that could not be characterized directly. Its chromatographic behavior suggested that its structure might correspond to that of **5**, analogous to the dithioformate iron complex (Scheme II) previously obtained by addition of borohydride to **2f** and **2g**.¹⁶ To support this structure for **5**, addition of dimethyl acetylenedicarboxylate was carried out and a red product, **7**, resulted. The structure of **7** is similar to that of the reaction products



of stable dithioformate iron complexes containing PMe_3 or PMe_2Ph with dimethyl acetylenedicarboxylate.¹⁶ The nature of the products **5** and **6** obtained by the reaction of **2h** with borohydride indicated that **2h** has a behavior toward hydride that is intermediate between that of **2a** ($L = \text{PPh}_3$) and **2f** or **2g** ($L = \text{PMe}_2\text{Ph}, \text{PMe}_3$), respectively. **2a** gave exclusively a complex, **3**, analogous to **6**, and **2f** and **2g** gave exclusively a complex analogous to **5**. Thus the behavior of **2h** seems mainly to be determined by the reduction potential, which indicates that electron transfer is less favored with **2h** than with **2a**.

The reduction of **2h** in THF with activated magnesium led to the formation of 30% of complex **6**, similar to the transformation of **2d** and **2e** into **3d** and **3e**. The reduction of **2h** with sodium amalgam led to a small amount (5%) of a yellow complex, **8**, and to 35% of a violet derivative, **9**. Complex **8** showed an infrared absorption at 1240 cm^{-1} typical of a FeCS group²³ in addition to two terminal carbonyl absorptions. Its structure is consistent with that of $\text{Fe}(\text{CS})(\text{CO})_2(\text{PR}_3)_2$ complexes that were previously obtained on treatment with Na/Hg of **2f** and **2g** that contain the more basic ligands PMe_2Ph and PMe_3 ,²³ respectively. The structure of the violet complex **9** corresponds to that of derivatives **4**, formed by Na/Hg reduction of **2a** ($L = \text{PPh}_3$), but containing two $\text{P}(\text{OMe})_3$ groups bonded to the iron center. Complex **9** probably results from **6** by elimination of one $\text{Fe}(\text{CO})_2(\text{P}(\text{OMe})_3)$ moiety, followed by substitution of one carbonyl by $\text{P}(\text{OMe})_3$.

Description of the X-ray Structures of 3a and 4a. Drawings of molecules **3a** and **4a** are shown in Figures 1 and 2, respectively. A selection of bond distances and bond angles is displayed in Table V for **3a** and Table VI for **4a**.

Molecule **3a** results from two $\text{Fe}(\text{CO})_2(\text{PPh}_3)$ moieties linked via an $\text{Fe}-\text{Fe}$ bond and held together by two sulfur atoms of a crosswise bridging ligand, $\text{S}_2\text{C}_2(\text{SMe})_2$. Thus, the $\text{S}_2\text{C}_2(\text{SMe})_2$ molecule sits upright on the "sawhorse" formed by the two $\text{Fe}(\text{CO})_2(\text{PPh}_3)$ units. This "sawhorse" has a wide open saddle as indicated by the large $\text{P}(2)-\text{Fe}(1)-\text{Fe}(2)$ and $\text{Fe}(1)-\text{Fe}(2)-\text{P}(1)$ angles of $152.8(5)^\circ$ and $152.5(5)^\circ$, respectively. The two $\text{Fe}(\text{CO})_2\text{PPh}_3$ fragments are almost eclipsed so that the plane containing the

(25) Neal Golovin, N.; Martiur Rahman, Md.; Belmonte, J. E.; Giering, W. P. *Organometallics* 1985, 4, 1981.

Table V. Bond Lengths (Å) and Angles (deg) for Fe₂S₂C₂(SMe)₂(CO)₄(PPh₃)₂ (3a)

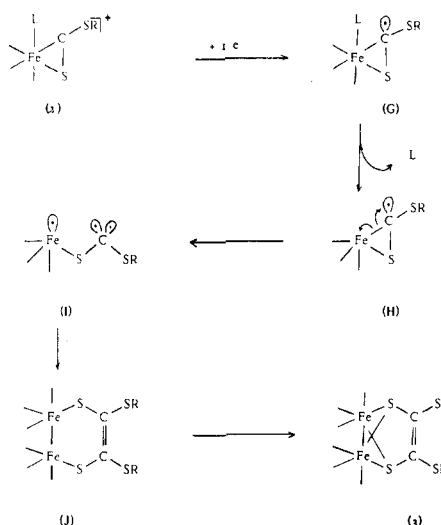
Fe(1)-Fe(2)	2.525 (2)	P(1)-C(9)	1.828 (7)
Fe(1)-S(1)	2.258 (2)	P(1)-C(15)	1.836 (7)
Fe(1)-S(2)	2.280 (2)	P(1)-C(21)	1.854 (6)
Fe(1)-P(2)	2.249 (2)	P(2)-C(27)	1.852 (6)
Fe(1)-C(1)	1.764 (7)	P(2)-C(33)	1.830 (6)
Fe(1)-C(2)	1.754 (6)	P(2)-C(39)	1.832 (6)
Fe(2)-S(1)	2.276 (2)	O(1)-C(1)	1.151 (7)
Fe(2)-S(2)	2.303 (2)	O(2)-C(2)	1.164 (7)
Fe(2)-P(1)	2.256 (2)	O(3)-C(3)	1.161 (8)
Fe(2)-C(3)	1.739 (7)	O(4)-C(4)	1.150 (8)
Fe(2)-C(4)	1.763 (8)	C(6)-C(7)	1.303 (8)
S(1)-C(6)	1.807 (6)		
S(2)-C(7)	1.798 (6)		
S(3)-C(7)	1.754 (6)		
S(3)-C(8)	1.783 (9)		
S(4)-C(5)	1.778 (10)		
S(4)-C(6)	1.733 (6)		
S(1)-Fe(1)-S(2)	79.31 (6)	P(1)-Fe(2)-C(3)	96.6 (3)
S(1)-Fe(1)-P(2)	101.00 (7)	P(1)-Fe(2)-C(4)	99.6 (2)
S(1)-Fe(1)-C(1)	92.0 (2)	C(3)-Fe(2)-C(4)	93.1 (3)
S(1)-Fe(1)-C(2)	150.9 (2)	Fe(1)-S(1)-Fe(2)	67.07 (6)
S(2)-Fe(1)-P(2)	106.60 (7)	Fe(1)-S(2)-Fe(2)	66.24 (6)
S(2)-Fe(1)-C(1)	154.4 (2)	C(7)-S(3)-C(8)	102.6 (3)
S(2)-Fe(1)-C(2)	87.9 (2)	C(5)-S(4)-C(6)	103.5 (4)
P(2)-Fe(1)-C(1)	98.6 (2)	Fe(1)-C(1)-O(1)	178.4 (6)
P(2)-Fe(1)-C(2)	98.7 (2)	Fe(1)-C(2)-O(2)	179.1 (6)
C(1)-Fe(1)-C(2)	92.4 (3)	Fe(2)-C(3)-O(3)	176.5 (7)
S(1)-Fe(2)-S(2)	78.46 (6)	Fe(2)-C(4)-O(4)	174.8 (7)
S(1)-Fe(2)-P(1)	102.71 (7)	S(1)-C(6)-S(4)	119.2 (4)
S(1)-Fe(2)-C(3)	92.5 (2)	S(1)-C(6)-C(7)	116.5 (4)
S(1)-Fe(2)-C(4)	156.2 (2)	S(2)-C(7)-S(3)	120.9 (4)
S(2)-Fe(2)-P(1)	105.50 (7)	S(2)-C(7)-C(6)	115.8 (5)
S(2)-Fe(2)-C(3)	157.4 (3)		
S(2)-Fe(2)-C(4)	87.7 (2)		

Table VI. Bond Lengths (Å) and Angles (deg) for Fe(PPh₃)(CO)₂(C₂S₄(CH₃)₂) (4a)^a

Fe-S(1)	2.163 (3)	S(4)-C(6)	1.820 (19)
Fe-S(2)	2.196 (3)	P-C11	1.840 (6)
Fe-P	2.244 (3)	P-C12	1.824 (7)
Fe-C(1)	1.788 (1)	P-C13	1.831 (7)
Fe-C(2)	1.776 (13)	O(1)-C(1)	1.165 (12)
S(1)-C(3)	1.701 (10)	O(2)-C(2)	1.127 (13)
S(2)-C(4)	1.708 (12)	C(3)-C(4)	1.390 (15)
S(3)-C(3)	1.750 (10)		
S(3)-C(5)	1.787 (18)		
S(4)-C(4)	1.767 (11)		
S(1)-Fe-S(2)	87.8 (1)	Fe-P-C11	113.8 (2)
S(1)-Fe-P	89.1 (1)	Fe-P-C12	117.5 (2)
S(1)-Fe-C(1)	150.8 (4)	Fe-P-C13	112.3 (2)
S(1)-Fe-C(2)	109.1 (3)	C11-P-C12	103.3 (3)
S(2)-Fe-P	168.6 (1)	C11-P-C13	105.1 (3)
S(2)-Fe-C(1)	87.4 (3)	C12-P-C13	103.6 (3)
S(2)-Fe-C(2)	98.9 (4)	Fe-C(1)-O(1)	179.0 (11)
P-Fe-C(1)	90.0 (3)	Fe-C(2)-O(2)	178.2 (10)
P-Fe-C(2)	92.5 (3)	S(1)-C(3)-S(3)	121.7 (7)
C(1)-Fe-C(2)	100.0 (5)	S(1)-C(3)-C(4)	118.0 (8)
Fe-S(1)-C(3)	107.9 (4)	S(3)-C(3)-C(4)	120.3 (8)
Fe-S(2)-C(4)	106.2 (4)	S(2)-C(4)-S(4)	121.8 (7)
C(3)-S(3)-C(5)	102.9 (6)	S(2)-C(4)-C(3)	119.2 (8)
C(4)-S(4)-C(6)	102.0 (7)	S(4)-C(4)-C(3)	119.0 (8)

^aThe phenyl rings were refined as rigid groups of *D*_{6h} symmetry with C-C distances fixed at 1.395 Å.

S₂C₂(SMe)₂ ligand is almost a plane of symmetry of the molecule **3a**. An orthogonal pseudosymmetry plane is also defined by the metal and phosphorus atoms. Divergences from ideal C_{2v} symmetry are mainly brought about by different orientations of the phenyl rings of the phosphines and the methyl groups attached to the uncoordinated sulfur atoms that are not coplanar with the C₂S₄ plane. The Fe₂S₂ core of the molecule has a butterfly-type structure with the Fe-Fe bond located along the hinge. The apex is occupied by the sulfur atoms S(1) and S(2).

Scheme V

The angle between the Fe(1)-Fe(2) and S(1)⋯S(2) vectors is 89.9 (4)°. The Fe-Fe bond length (2.525 (2) Å) compares well with other Fe-Fe single bond distances found in other complexes with similar frameworks such as in (CO)₃Fe-(Ph₂C₂S₄)Fe(CO)₃²⁶ (2.507 (5) Å). The angles Fe(1)-S(1)-Fe(2) (67.07 (6)°) and Fe(1)-S(2)-Fe(2) (66.24 (6)°) are acute; the Fe-S, C-S, and C-C distances in the above reference²⁶ and in **3a** compare as follows: 2.26 (1) (av) vs 2.28 (2) Å; 1.78 (3) vs 1.80 Å; 1.35 (1) vs 1.31 (1) Å, respectively.

Molecule **4a** contains a five-coordinate iron atom bonded to one PPh₃ ligand, two carbonyl groups, and two sulfur atoms of the S₂C₂(SMe)₂ ligand. The large values of the two angles C(1)-Fe-S(1) and P-Fe-S(2) (150.8 (4) and 168.6 (1)°, respectively) indicate that the coordination polyhedron approximates a square pyramid. The Me₂C₂S₄ ligand chelates the metal at basal sites of the pyramid, and the C(2)-O(2) carbonyl occupies the apex. From an alternate viewpoint the complex can be described as assembled from the hemioctahedral L₃M fragment, (PPh₃)-(CO)₂Fe, and a molecule of Me₂C₂S₄, which is essentially planar except for the terminal methyl groups (the out-of-plane displacement of C(6) is as much as 0.76 Å). The Fe-S distances (2.18 (2) Å) are significantly shorter in **4a** than in **3a** (2.28 (2) Å), indicating a great deal of electron delocalization within the Fe-S-C-C-S metallacycle. This is also reflected in the C-C bond that is much longer in **4a**, 1.390 (15) Å vs 1.35 (2) Å in (Ph₂C₂S₄)Fe(CO)₆²⁶ and 1.303 (8) Å in **3a**. Concomitantly, the (Fe)S-C distances decrease in the reverse order: 1.802 (6) Å in **3a**, 1.775 Å in (CO)₃Fe(Ph₂C₂S₄)Fe(CO)₃²⁶ and 1.704 (12) Å in **4a**. These trends are consistent with a stronger electron release from the S₂C₂(SMe)₂ ligand toward the iron atom in **3a** than in **4a**.

Discussion of the Mechanism. An attempt to rationalize the formation of complexes **3** from cations **2** is provided by Scheme V. (i) The first step corresponds to a one-electron transfer, either from borohydride or from sodium amalgam, to the cation **2**. The large difference between the reduction potential (*E*_c) of cations **2** (Table IV) and the potential of the 1/2 H₂/H⁻ system (*E*^o = -2.25 V vs SCE) allows electron transfer to occur from the hydride. This reduction process is faster with sodium amalgam, which shows a more negative potential (*E*^o (Na⁺/Na) = -2.96 V vs SCE). According to the MO dia-

gram for a metal/ η^2 -CS₂ interaction,¹² the electron is expected to be transferred to a π_{\perp}^* antibonding MO of CS₂, centered mainly on the carbon atom, as indicated in structure G. This orbital energy is slightly lower in cation **2** than in its precursor Fe(η^2 -CS₂) derivative. (ii) The second step may be related to the elimination of one PPh₃ group from G and the formation of the unsaturated species H. Indeed, we have shown²⁷ that although the Ph₃P groups are strongly bonded to iron in cation **2**, these groups are immediately displaced by PMe₃ groups on electrocatalytic reduction to afford complex **2f**. Under conditions corresponding to that of **2** → **3** but in the presence of PMe₃ the dimerization into **3** was not observed. Instead substitution of PPh₃ groups occurs. (iii) The electronic unsaturation at the iron center in species H may promote the homolytic cleavage of the Fe-C(SR) bond to give species I.²⁸ (iv) The nature of I would then explain its dimerization into J. (v) The intermediate J would become **3** by coordination of each sulfur atom to the second metal center, allowing the iron atoms to reach their 18-electron configuration.

Conclusion

The above results show an example of the striking influence of ancillary ligands on the reactivity of a metal-

(27) Fillaut, J. L.; Touchard, D.; Dixneuf, P., unpublished results.

(28) Homolysis of the M-C bond in Rh(η^2 -CS₂) complexes has already been shown and rationalized¹² on account of an intended but avoided crossing of two levels centered on the metal and carbon atoms, respectively. In that case the conditions were the proper ones for the formation of a diradical species. In the case of the species H the M-C dissociation pathway is complicated by the fact that the carbon is taken as having already a radical character.

substrate moiety. The reaction of Fe(η^2 -CS₂R)(CO)₂(L)₂⁺ cations (**2** (L = PPh₃ or P(OMe)₃), with either borohydride or sodium amalgam, shows that the nature of the reaction products depends not only on the electron donor capability of L but also on the Fe-L lability and the reduction potential of the cation. The latter is related to both steric and electronic effects of L. Our study of cations **2** shows that the influence of L = PPh₃ is to favor monoelectronic processes, and this leads to reactions different from those with L = PMe₃. By contrast, L = P(OMe)₃ shows, as indicated by its reduction potential and not by its electronic effect, a behavior that is in between that of L = PPh₃ and that of L = PMe₃. It is thus shown that the nature of L in cations **2** determines the behavior of the Fe(η^2 -CS₂R)⁺ moiety.

Acknowledgment. This work was supported by CNRS and the "Progetto bilaterale" approved by Italian CNR.

Registry No. 1, 64424-68-6; **2a** (X = I), 72598-18-6; **2a** (X = PF₆), 71004-19-8; **2b**, 111002-63-2; **2c**, 110904-33-1; **2d**, 110904-35-3; **2e**, 110904-37-5; **2h**, 71004-17-6; **3a**, 97390-97-1; **3b**, 110904-38-6; **3c**, 110904-39-7; **3d**, 110904-40-0; **3e**, 110904-41-1; **4a**, 97390-96-0; **4b**, 110904-42-2; **4c**, 110904-43-3; **4d**, 110904-44-4; **4e**, 110904-45-5; **5**, 110904-48-8; **6**, 110904-46-6; **7**, 110904-49-9; **8**, 110904-47-7; **9**, 97403-35-5; Fe(η^2 -CS₂)(CO)₂(P(OMe)₃)₂, 64424-66-4; pulegone, 89-82-7; benzylideneacetone, 122-57-6; dimethyl acetylenedicarboxylate, 762-42-5.

Supplementary Material Available: Anisotropic thermal parameters for the structure of **3a** (Table S3) and **4a** (Table S4) (3 pages); listings of observed and calculated structure factor amplitudes (Tables S1 and S2) (19 pages). Ordering information is given on any current masthead page.

Kinetics of Alkyldisilane Pyrolyses and Heats of Formation of Methylsilylenes

R. Walsh

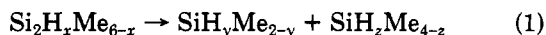
Department of Chemistry, University of Reading, Whiteknights, Reading RG6 2AD, U.K.

Received April 22, 1987

It is shown that Arrhenius parameters for various methylated disilane decomposition reactions are not consistent with recent time-resolved rate measurements for SiH₂ and SiMe₂. Possible reasons for this are discussed, and existing data are reassessed to provide heats of formation of 26 (± 2) and 44 (± 3) kcal mol⁻¹ for SiMe₂ and SiHMe, respectively.

Introduction

Silylenes, SiH_nMe_{2-n} (*n* = 0, 1, or 2) are implicated as intermediates in many high-temperature organosilane reactions.¹ Mechanistic understanding of such reaction systems has reached the point where analytical and kinetic data are routinely fitted with kinetic modeling schemes.^{2,3} Much information on the behavior of silylenes has come from studies of the thermal decompositions of the methylidisilanes



where *x* = 0-6, *y* = 0-2, and *z* = *x*-*y*. For example, a knowledge of the activation energy *E*₁ for such a process, combined with the reverse activation energy *E*₋₁, leads to $\Delta H_{1,-1}$. The heat of formation of the silylene, ΔH_f° (SiH_yMe_{2-y}), can then be obtained provided the heats of formation of the silane SiH₂Me_{4-z} and disilane Si₂H_xMe_{6-x} are known.

Several gas-phase kinetic studies of methylidisilanes have been carried out,⁴⁻⁷ and activation energies obtained. Until

(1) Gaspar, P. P. *Reactive Intermediates* (Wiley) 1978, 1, 229; 1981, 2, 335; 1985, 3, 333.

(2) See for example: Davidson, I. M. T.; Hughes, K. J.; Scampton, R. *J. J. Organomet. Chem.* 1984, 272, 11.

(3) See for example: Rickborn, S. F.; Rogers, D. S.; Ring, M. A.; O'Neal, H. E. *J. Phys. Chem.* 1986, 90, 408.

(4) Vanderwielen, A. J.; Ring, M. A.; O'Neal, H. E. *J. Am. Chem. Soc.* 1975, 97, 993.

(5) Davidson, I. M. T.; Matthews, J. I. *J. Chem. Soc., Faraday Trans. 1* 1976, 72, 1403.